On mathematical modeling of the transmission of Grapevine leafroll-associated virus 3 by the vine mealybug, *Planococcus ficus*

Michael Chapwanya* & Erin Kenyon
Department of Mathematics & Applied Mathematics, University of Pretoria, Pretoria 0002, South Africa

Abstract

Grapevine leafroll disease (GLD) is the most common and economically destructive grapevine viral disease in South African vineyards and throughout the world. There are many GLD-associated virus variants with Grapevine leafroll-associated virus 3 (GLRaV-3) being the main causative agent of GLD. The vine mealybug, *Planococcus ficus*, is the most widespread and problematic vector of GLRaV-3. Roguing, pesticides and sanitary measures are common control strategies used in South African vineyards. In this paper, we propose an age-structured mathematical model for the transmission of (GLRaV-3) by *Planococcus ficus* in the South African context. The model is investigated in terms of the transmission thresholds and control strategies. A simplified model is used to shed light into the qualitative dynamics of transmission and assess the effectiveness of roguing as the main control strategy for GLRaV-3 spread.

1 Introduction

Most plant viruses are vector-borne. The modes of pathogen transmission is based on characteristics of virus–vector interactions. Viruses that replicate within insects are transmitted in a propagative manner and those that do not are nonpersistently, semipersistently, or circulatively (persistently) transmitted. Grapevine Leafroll Disease (GLD) is the most economically damaging grapevine viral disease [1–3], being responsible for 60% of yield losses in grape production [3]. It affects grape quality and vine health, often resulting in shorter vineyard life spans as well as the late maturity of grapes, all of which affect the sale to market and overall wine quality. The disease is found in almost every grape growing region in the world, in particular, in the wine making industry in South Africa where the infection rate is disastrously high [4, 5].

GLD is caused by a number of grapevine leafroll-associated virus types [5, 2]. This paper will focus on grapevine leafroll-associated virus 3 (GLRaV-3), as it is the main causative agent of GLD and a recent study done by the ARC-Plant Protection Research Institute found GLRaV-3 in all surveyed vines whenever GLD symptoms were observed in the area. GLRaV-3 has been dispersed throughout the world due to the trade and propagation of infected plant material [5]. Recent spread is due to vegetative propagation, mealy bug and soft scale species [6–8].

*Corresponding author. m.chapwanya@up.ac.za; Tel.: +27 12 420 2837; Fax.: +27 12 420 3893

The symptoms of GLD vary greatly depending on cultivar, season and climate [9, 2, 5, 1]. The symptoms of red and white varieties differ markedly [2, 9, 5]. Red varieties typically display leaf reddening with green venation while some develop a uniform red colour [9, 1, 5]. The display of symptoms in white varieties, when visible, is much less conspicuous with the area around the veins becoming slightly chlorotic, turn pale yellow or yellow-white in colour [9, 2]. These leaf symptoms first appear mid-Summer becoming more obvious in Autumn. By late Autumn the leaves of most varieties, red and white, show a downward rolling of the leaf margins, see Fig. 1.

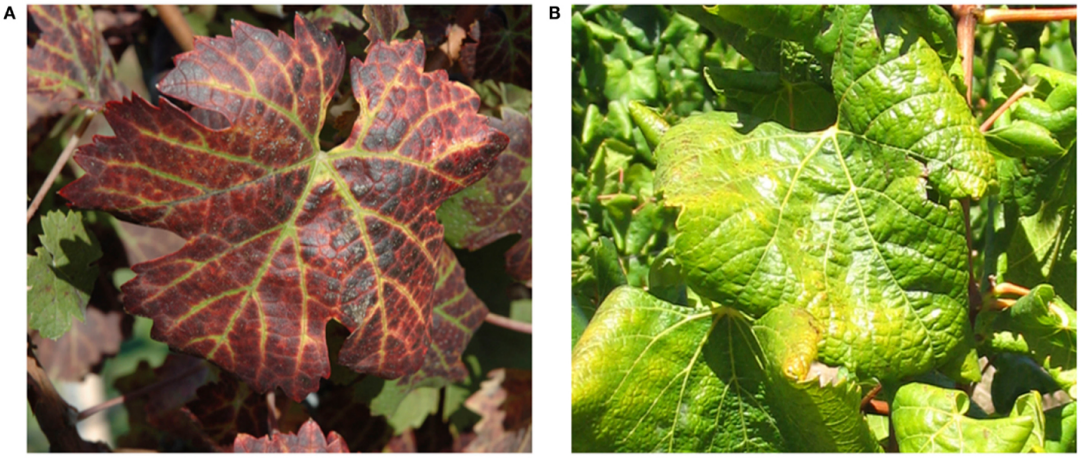

Figure 1: A: Typical symptoms of GLD in red variety, B: Typical symptoms of GLD in white variety [2].

Pl. ficus (Signoret), the vine mealybug, is the most widespread and problematic vector of GLRaV-3 in South Africa [10, 11]. For this reason, the transmission of GLRaV-3 by *Pl. ficus* is the focus of this paper. *Pl. ficus* was first discovered as a key vineyard pest in South Africa in 1914, but was wrongly identified as *Planococcus citri* (Rosso) (the citrus mealybug) at the time [12, 10]. It was subsequently identified as *Pl. ficus* in 1975 [12, 10], and was believed to have been introduced to South Africa through imported plant material. To date, it is found in most grape growing regions of the world. High infestations of *Pl. ficus* can cause early leaf loss and resultant weakening of vines, [10]. In addition to the transmission of GLRaV-3, mealybugs cause direct damage to vines by sucking phloem sap and, indirectly, by excreting large amounts of honeydew which promotes the growth of sooty mould, thereby reducing the photosynthetic activity, see Fig. 2. The mealybugs and honeydew on the grapes reduce the market value of the grape cluster [9, 10]. Heavy infestations can even cause vine death through the early loss of leaves [10].

An understanding of the transmission of GLRaV-3 by *Pl. ficus* is important when formulating the mathematical model. These models can be used to predict the behaviour of disease transmission and evaluating the effectiveness of control strategies [13]. GLRaV-3 is transmitted in a semi-persistent manner with *Pl. ficus* only retaining the virus for a short period of time [14, 15]. When the mealybug moults it loses its infection with GLRaV-3 and becomes susceptible once more [14, 7]. GLRaV-3 is also not transovarially transmitted from adult mealybugs to eggs, i.e., the adult does not pass on the virus to her offspring, [15]. The inoculation access period and the acquisition access period of GLRaV-3, i.e., the amount of time it takes for the

Figure 2: *Planococcus ficus* on grapevine stalk.

vector to transmit or become infected, is short and so there is no latent period [14, 15]. *Pl. ficus* has a very high transmission efficiency of 70% and a single nymph is capable of infecting several healthy grapevines.

The life stage of *Pl. ficus* has a significant effect on its transmission efficiency of GLRaV3 [15], see Fig. 3. The dispersal stage is when the first instars (crawlers) emerge and are easily spread by birds, ants and the wind, and so are the main source of GLRaV-3 transmission [15–17, 9]. They moult into second and then third instars, each resembling the previous stage except for the increasing size and amount of wax secretion [9]. With each moult the instars become larger and less mobile, thus reducing the chances of transmission [9, 17]. The development of the male and female *Pl. ficus* differ in their final life stages [17]. From the third instar, the female *Pl. ficus* becomes an adult. The male however moults into a pre-pupa, pupa and then a winged adult male. This is an important distinction to bear in mind as the adult male has no mouth piece and so cannot transmit the virus. All stages except the males in the final stages (pre-pupa, pupa and adult) have the ability to transmit the virus [7]. Moreover, it is very unlikely that the female adult will transmit the virus in field conditions due to her sedentary behaviour [15, 9]. Hence, in this work, we assume the adult (male and female) do not transmit the virus. In particular, as argued in [15], first instars are the most mobile stage of mealybugs and under field conditions, the spread of GLRaV-3 may be largely driven by this life stage. The almost year-long warm climate in most grape-growing regions in South Africa leads to overlapping generations of *Pl. ficus*, resulting in multiple life stages being present at any one time.

There are many different GLD control strategies put in place in South Africa. First and foremost, the provision of healthy certified planting material [5]. If the certified material comes from areas at risk of GLD re-infection there is a small possibility of planting infected material and so, once planted systemic insecticides are applied, and roguing of GLD-infected vines in the newly established vineyards [5]. South African commercial vineyards control GLD through roguing of infected vines and mealy bug control methods such as sanitation measures, for example, washing implements when moving from infected vineyards to healthy ones [5, 18]. In this paper we propose a mathematical model for the transmission of GLRaV-3 by the vine

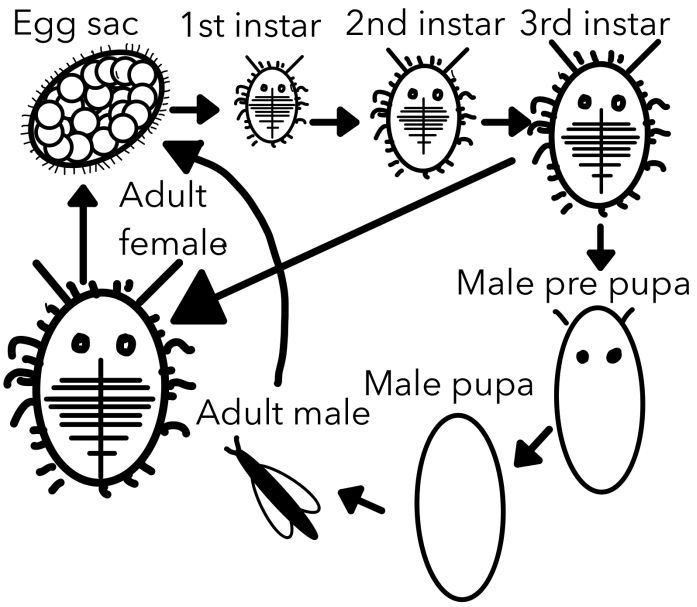

Figure 3: Simplified life cycle of *Pl. ficus*.

mealybug, *Pl. ficus*, taking into account the first 3 developmental stages of the vector. The model is later simplified through the exclusion of the age-structure and only considering the transmission of GLRaV-3 by all developmental stages as a single vector class. This reduced model allows us to better analyse and make conclusions about the dynamics of the system.

2 The model formulation

The age-structured GLD model is designed by splitting the total vector population (*Pl. ficus*), at time t, denoted by $V(t)$, into mutually-exclusive sub-populations of susceptible $S_i(t)$ and infected $I_i(t)$, for $i = 1, 2, 3$. To this end, we have

$$V(t) = S_1(t) + I_1(t) + S_2(t) + I_2(t) + S_3(t) + I_3(t).$$

The male and female mealybug have the same early developmental stages from eggs: first instars ($V_1(t) = S_1(t) + I_1(t)$), second instars ($V_2(t) = S_2(t) + I_2(t)$) and third instars ($V_3(t) = S_3(t) + I_3(t)$). The females become adults after the third instars, but the male goes through a pre-pupal, pupal and adult stage. The male would not be able to transmit the virus while in his pre-pupal and pupal stage as it would not be feeding. The adult male emerges from its pupa without a mouth piece and is thus unable to transmit the virus. We assume the female adults are not capable of transmitting the virus in the field due to their sedentary behaviour [15]. For this reason, their dynamics are not included in the model. The first instars morph into second instars at a rate (γ_1), the second instars morph into third instars at a rate (γ_2), and the third instars morph into adults at a rate (γ_3). The virus leaves the mealybug's system when it moults and as a result there is no movement from the early infected instars to the later infected instars [14, 7].

The total plant biomass of the vineyard is denoted by $P(t)$, and also subdivided into mutually-exclusive sub-populations of the susceptible and healthy biomass $S_p(t)$, and the infected biomass $I_p(t)$. We have

$$P(t) = S_p(t) + I_p(t).$$

The expression of symptoms varies by season and variety, with some vines being infected but not showing symptoms. The transmission process is summarised in Fig. 4

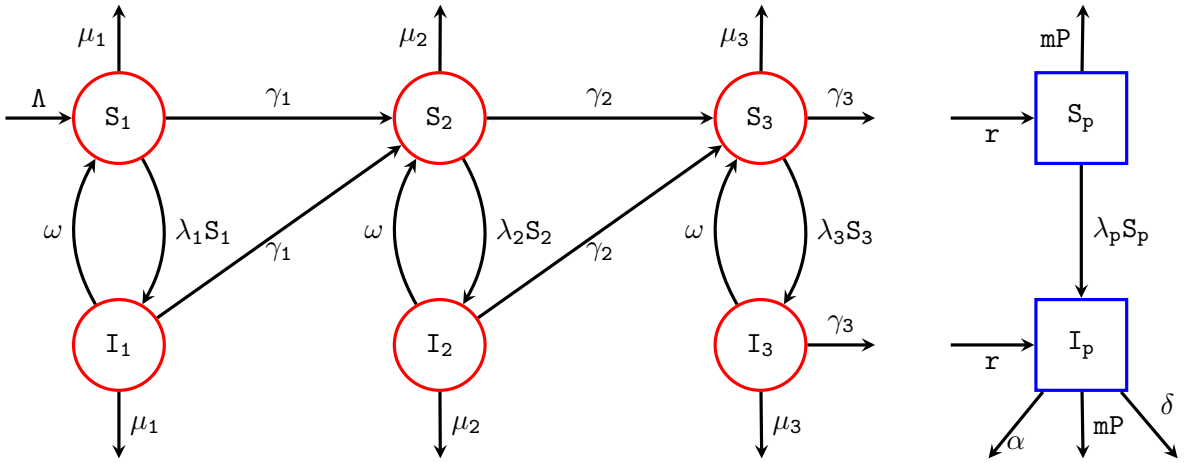

Figure 4: Schematic diagram of the the GLD disease transmission.

The vector population is generated by birth at a constant rate of Λ, moving into the susceptible compartment of the first instar stage. It is decreased by maturation to the second instar at the rate of γ_1, and natural death at the rate μ_1. The younger they are the more vulnerable they are, and so would have different mortality rates for the different life stages. Denoting β_{pj}, for $j = 1, 2, 3$, the contact rate per unit time, between infectious plants and susceptible first instars, we have, the force of infection for instar j, given by

$$\lambda_j = \beta_{pj} I_p.$$

As motivated before, we assume only the first, second and third instars are capable of transmitting the virus since the adult male does not feed and the sedentary behaviour of the adult female. GLRv-3 is transmitted by the vector in a semi-persistent manner - the vector population becomes susceptible again at the rate of ω (which, for simplification, is assumed to be the same for all life stages), [15, 11]. Thus

$$\begin{aligned} \frac{dS_1}{dt} &= \Lambda - \lambda_1 S_1 - (\gamma_1 + \mu_1) S_1 + \omega I_1, \\ \frac{dI_1}{dt} &= \lambda_1 S_1 - (\gamma_1 + \mu_1 + \omega) I_1. \end{aligned} \tag{2.1}$$

We remark that the choice for constant recruitment Λ, is for mathematical convenience. Other density dependent choices can also be used. Assuming γ_2 is rate of maturation of the second

instar into the third instar, and μ_2 the natural death rate of the second instar, we have

$$\begin{aligned}\frac{dS_2}{dt} &= \gamma_1 S_1 - \lambda_2 S_2 - (\gamma_2 + \mu_2) S_2 + \omega I_2 + \gamma_1 I_1,\\ \frac{dI_2}{dt} &= \lambda_2 S_2 - (\gamma_2 + \mu_2 + \omega) I_2.\end{aligned} \tag{2.2}$$

Denoting by γ_3, the maturation rate of the third instar into adulthood, we also have

$$\begin{aligned}\frac{dS_3}{dt} &= \gamma_2 S_2 - \lambda_3 S_3 - (\mu_3 + \gamma_3) S_3 + \omega I_3 + \gamma_2 I_2,\\ \frac{dI_3}{dt} &= \lambda_3 S_3 - (\gamma_3 + \mu_3 + \omega) I_3.\end{aligned} \tag{2.3}$$

New biomass population is generated through plant replacement. Though considerable efforts have been made in the use of healthy certified and disease-resistant plants, for the purpose of assessing the effectiveness of these control strategies, we assume both susceptible and infected plants are used for new biomass at a constant rate r. GLRaV-3 does cause direct loss in the grapevine biomass at the rate α, and we also have loss in biomass due to respiration, transpiration and maintenance, and this is assumed to be same in each of the epidemiological class. Of particular interest, the virus does greatly reduce the growth rate and yield. We propose the following for the plant biomass

$$\begin{aligned}\frac{dS_p}{dt} &= rS_p - mPS_p - \lambda_p S_p,\\ \frac{dI_p}{dt} &= rI_p - mPI_p + \lambda_p S_p - (\delta + \alpha) I_p,\end{aligned} \tag{2.4}$$

where $\lambda_p = \sum_{i=1}^{3} \beta_{ip} I_i$ with β_{ip} the contact rate (per unit time) between infectious vectors and susceptible plants. In addition, $m \in [0, 1]$ is the plant biomass loss due to respiration, transpiration and maintenance (which is assumed to be the same for all compartments), and δ is the roguing rate. The term $-mPI_p$ is multiplied by P to include interaction with both healthy and infected plants, see for example [19].

To the best of our knowledge, the proposed model equations model (2.1), (2.2) and (2.3), are new and it is the first time a GLRaV-3 virus transmission model of this nature has been investigated. We have tried to make the model as generic as possible, so that it is applicable to other age-structured vector-borne plant diseases, [19].

2.1 Parameter selection

GLRv-3 is transmitted by *Pl. ficus* in a semi-persistent manner with loss of vector infectivity over a period of days. Acquisition and inoculation occur within $1h$ of plant access, with no observable latent period [9]. Under laboratory conditions transmission efficiency of GLRaV-3 by *Pl. ficus* was ca. 10% per individual per day [15]. The work [11] reported infection rates of grapevine plants ranging between 6% to 16% per day for first- to second-instar nymphs.

Developmental times of *Pl. ficus* varies across the 3 instars depending on temperature conditions. Developmental time for each life stage decreased with increasing temperature, but

remains constant above and below certain threshold values [20]. For instance [21] reported 2.20 - 5.60 days for the first instar, 5.50 - 10.86 days for the second instar and 6.42 - 16.30 days for the third instar. This is consistent with the work of [22] who also reported that adult females lived from 27.64 days at 30^oC to 63.70 days at 20^oC, whereas males lived 1.66 - 7.55 days, respectively. Taking the reciprocal of these life spans, we have the estimates, $\gamma_1 = [0.179, 0.455]$ day^{-1}, $\gamma_2 = [0.0921, 0.182]$ day^{-1}, and $\gamma_3 = [0.0613, 0.156]$ day^{-1}, where the $[*, *]$ denotes the interval of validity for the specified parameter. As reported in [23], a female can lay from 300 to 600 eggs in her life period. Taking into consideration the adult *Pl. ficus* life span, that will give an average of [10,22] eggs per day.

Parameters	Description	Value	Unit	Source
Λ	Vector birth rate	[10,22]	eggs.day^{-1}	[23]
ω	Recovery rate	0.333	day^{-1}	[14]
μ_1	Natural mortality, 1st instars	[0,0.0424]	day^{-1}	[22]
μ_2	Natural mortality, 2nd instars	[0,0.0382]	day^{-1}	[22]
μ_3	Natural mortality, 3rd instars	[0,0.0109]	day^{-1}	[22]
γ_1	Maturation rate of 1st instar	[0.179,0.455]	day^{-1}	[21]
γ_2	Maturation rate of 2nd instar	[0.0921,0.182]	day^{-1}	[21]
γ_3	Maturation rate of 3rd instar	[0.0613,0.156]	day^{-1}	[21]
β_{pi}	Acquisition rate	[10^{-4},0.0286]	biomass^{-1}day^{-1}	[11]
β_{ip}	Infection rate	[10^{-4},0.0286]	vector^{-1}day^{-1}	[11]
r	Biomass growth rate	[0.002,0.004]	day^{-1}	estimated
m	Biomass maintenance	[0,1]	biomass^{-1}day^{-1}	estimated
δ	Roguing rate	[0,1]	day^{-1}	estimated
α	Loss of Biomass due to virus	[0,1]	day^{-1}	estimated

Table 1: Summary of parameters values. The subscript $i = 1, 2, 3$, denoting the first-, second-, and third-instars, respectively.

In [22], the authors investigated the development and longevity of female *Pl. ficus* at different temperatures. The natural mortality for first-, second-, and third-instars were found to be influenced by temperature. Using their data, we estimate the natural mortality as follows: $\mu_1 = [0, 0.0424]$ day^{-1}, $\mu_2 = [0, 0.0382]$ day^{-1}, and $\mu_3 = [0, 0.0109]$ day^{-1}. Acquisition and inoculation access periods for *Pl. ficus* were investigated in [14]. *Pl. ficus* nymphs can acquire GLRaV-3 after an acquisition access periods of as little as 15 min and transmit the virus to healthy plants, and they can inoculate healthy plants after an inoculation access periods of 15 min. They retained the virus for at least three days when feeding on virus-free vines or starving. We summarise these, and all the parameter values in Table 1.

Not much information is available in the literature regarding the grapevine biomass parameters, i.e., r, m, δ and α. Grapes are produced in South Africa from mid-November to mid-April, with an average growth of 1–1.5 inches per day during this period. Assuming mature unpruned grape vine can grow to 115 feet in length, we estimate the growth rate to be [0.002 - 0.004] per

day. This number is an average based on the assumption that we have 10 branches of 115 feet each. Biomass maintenance parameter is assumed to be in the range $m \in [0,1]$ biomass^{-1}day^{-1}. Roguing has been used, ranging from replacing two within-row adjacent vines on each side with clean vines, to the total replacement of the whole vineyard [24]. Hence, based on the definition of the parameters, we estimate the roguing rate in the range $[0,1]$ and estimate the grapevine loss due to virus in the range [0,1] per day. However, studies suggest vineyard replanting would be the optimal strategy for disease prevalence of more than 25%. The specific selection of baseline parameter values is given in Table 2.

3 Basic properties

Based on the above derivations and assumptions, the age structured model for the transmission dynamics of GLRv-3 is summarised by the following differential equation model

$$\begin{aligned}
\frac{dS_1}{dt} &= \Lambda - \lambda_1 S_1 - (\gamma_1 + \mu_1)S_1 + \omega I_1,\\
\frac{dI_1}{dt} &= \lambda_1 S_1 - \rho_1 I_1,\\
\frac{dS_2}{dt} &= \gamma_1 S_1 - \lambda_2 S_2 - (\gamma_2 + \mu_2)S_2 + \omega I_2 + \gamma_1 I_1,\\
\frac{dI_2}{dt} &= \lambda_2 S_2 - \rho_2 I_2,\\
\frac{dS_3}{dt} &= \gamma_2 S_2 - \lambda_3 S_3 + \omega I_3 - (\mu_3 + \gamma_3)S_3 + \gamma_2 I_2,\\
\frac{dI_3}{dt} &= \lambda_3 S_3 - \rho_3 I_3,\\
\frac{dS_p}{dt} &= rS_p - mPS_p - \lambda_p S_p,\\
\frac{dI_p}{dt} &= rI_p - mPI_p + \lambda_p S_p - (\delta + \alpha)I_p.
\end{aligned} \tag{3.1}$$

and the corresponding flow chart given in Fig. 4. Here, for convenience, $\rho_i = \gamma_i + \mu_i + \omega$ for $i = 1,2,3$. Adding all the equations in (3.1), we get

$$\frac{dV}{dt} = \Lambda - (\mu_1 V_1 + \mu_2 V_2 + \mu_3 V_3) - \gamma_3 V_3 \leq \Lambda - \mu V, \quad V(0) = V_0 \geq 0, \tag{3.2}$$

where $\mu = \min\{\mu_1, \mu_2, \mu_3\}$. Similarly, adding equations in (2.4), gives

$$\frac{dP}{dt} = rP - mP^2 - (\delta + \alpha)I_p \leq rP - mP^2, \quad P(0) = P_0 \geq 0. \tag{3.3}$$

From (3.2) and (3.3) we deduce that $V(t) \leq V^* = \dfrac{\Lambda}{\mu}$ and $P(t) \leq P^* = \dfrac{r}{m}$, respectively, when $t \to \infty$. We notice that, since $V_0 \geq 0$ and $P_0 \geq 0$, then $V(t) \geq 0$ and $P(t) \geq 0$, respectively, for all $t > 0$. Hence the solution of (3.2) and (3.3) for any initial condition in $\Omega_{V,P}$ remains in $\Omega_{V,P}$ where $\Omega_{V,P} = [0, V^*] \times [0, P^*]$.

Next, through the following result, we show that the model is mathematically and biologi-

cally well posed in

$$\Omega = \left\{(S_1, I_1, S_2, I_2, S_3, I_3, S_p, I_p) \in \mathbb{R}^8_+ : [0, V^*]^6 \times [0, P^*]^2\right\}. \tag{3.4}$$

Theorem 1. *Assuming that all initial conditions lie in Ω, then system (3.1) has a unique solution that remains in Ω for all positive time t.*

Proof. The right hand side of the system is a continuously differentiable map (C^1), and we can apply the Cauchy-Lipschitz theorem in [25] to conclude that the system has a unique maximal solution. Next we rewrite the system in the form

$$\frac{dx}{dt} = A(x)x + b,$$

where $x = (S_1, I_1, S_2, I_2, S_3, I_3, S_p, I_p)^t$, $b = (\Lambda, 0, 0, 0, 0, 0, 0, 0)^t \geq 0$, and matrix $A(x)$ given by

$$A(x) = \begin{pmatrix} -\kappa_1(x) & \omega & 0 & 0 & 0 & 0 & 0 & 0 \\ \lambda_1(x) & -\rho_1 & 0 & 0 & 0 & 0 & 0 & 0 \\ \gamma_1 & \gamma_1 & -\kappa_2(x) & \omega & 0 & 0 & 0 & 0 \\ 0 & 0 & \lambda_2(x) & -\rho_2 & 0 & 0 & 0 & 0 \\ 0 & 0 & \gamma_2 & \gamma_2 & -\kappa_3(x) & \omega & 0 & 0 \\ 0 & 0 & 0 & 0 & \lambda_3(x) & -\rho_3 & 0 & 0 \\ 0 & 0 & 0 & 0 & 0 & 0 & d(x) - \lambda_p(x) & 0 \\ 0 & 0 & 0 & 0 & 0 & 0 & \lambda_p(x) & d(x) - (\delta + \alpha) \end{pmatrix}$$

where $\kappa_i(x) = \lambda_i(x) + \gamma_i + \mu_i$ for $i = 1, 2, 3$, and $d(x) = r - mP$. We see that $A(x)$ is a Metzler matrix, i.e., all of the off diagonal entries are non-negative for all $x \in \Omega$, and the exponential of a Metzler matrix is nonnegative. Therefore, since $x(0) \geq 0$, then $x(t) \geq 0$ for all $t > 0$. Thus Ω is invariant and the model is well posed, both mathematically and biologically. □

3.1 Model thresholds

The basic reproduction number, $\mathcal{R}_0$, is the expected number of secondary infections one typically infected individual would generate in a completely susceptible population [26]. We establish the local stability of the disease-free equilibrium using the next generation operator method, [27, 28]. We set the right hand side of system (3.1) to zero, to obtain the disease-free equilibrium, given by $E_{\text{DFE}} = (V_1^*, 0, V_2^*, 0, V_3^*, 0, P^*, 0)^t$, where

$$V_1^* = \frac{\Lambda}{\gamma_1 + \mu_1}, \quad V_2^* = \frac{\gamma_1 V_1^*}{\gamma_2 + \mu_2}, \quad V_3^* = \frac{\gamma_2 V_2^*}{\gamma_3 + \mu_3}. \tag{3.5}$$

Remark 1. *For later reference, we note the following: adding the first two equations in (3.1), we obtain*

$$\frac{dV_1}{dt} = \Lambda - (\gamma_1 + \mu_1)V_1.$$

A similar procedure for the third and forth equations, followed by the fifth and sixth equations

gives

$$\frac{dV_2}{dt} = \gamma_1 V_1 - (\gamma_2 + \mu_2)V_2, \quad \frac{dV_3}{dt} = \gamma_2 V_2 - (\gamma_3 + \mu_3)V_3,$$

respectively. From these equations we deduce that $V_1 \to V_1^*$, $V_2 \to V_2^*$ *and* $V_3 \to V_3^*$ *when* $t \to \infty$ *as stated in* (3.5).

Considering only the equations where the infection progress, we write

$$\frac{dX}{dt} = \mathcal{F}(X) - \mathcal{V}(X), \tag{3.6}$$

where $X = (I_1, I_2, I_3, I_p)^t$, and

$$\mathcal{F}(X) = \begin{pmatrix} \beta_{p1} I_p S_1 \\ \beta_{p2} I_p S_2 \\ \beta_{p3} I_p S_3 \\ \lambda_p S_p + r I_p \end{pmatrix}, \quad \text{and} \quad \mathcal{V}(X) = \begin{pmatrix} \rho_1 I_1 \\ \rho_2 I_2 \\ \rho_3 I_3 \\ (\alpha + \delta) I_p + m P I_p \end{pmatrix}.$$

The terms $\mathcal{F}(X)$ and $\mathcal{V}(X)$ distinguishes the rate of appearance and disappearance of infections respectively. The next generation matrix is given by NGM$=J_{\mathcal{F}} J_{\mathcal{V}}^{-1}$ where

$$J_{\mathcal{F}} = \begin{pmatrix} 0 & 0 & 0 & \beta_{p1} V_1^* \\ 0 & 0 & 0 & \beta_{p2} V_2^* \\ 0 & 0 & 0 & \beta_{p3} V_3^* \\ \beta_{1p} P^* & \beta_{2p} P^* & \beta_{3p} P^* & r \end{pmatrix},$$

and

$$J_{\mathcal{V}} = \begin{pmatrix} \rho_1 & 0 & 0 & 0 \\ 0 & \rho_2 & 0 & 0 \\ 0 & 0 & \rho_3 & 0 \\ 0 & 0 & 0 & r + \alpha + \delta \end{pmatrix},$$

are the Jacobian matrices of $\mathcal{F}(X)$ and $\mathcal{V}(X)$ respectively, evaluated at the disease-free equilibrium point. The basic reproduction number, $\mathcal{R}_0$, is defined as the spectral radius of NGM at the disease-free equilibrium. This gives

$$\mathcal{R}_0 = \frac{\mathcal{R}_{0v}}{2} + \sqrt{\frac{\mathcal{R}_{0v}^2}{4} + \mathcal{R}_{0pv}}, \tag{3.7}$$

where

$$\mathcal{R}_{0v} = \frac{r}{r + \alpha + \delta},$$

represents vertical transmission (transmission through the production of new plant biomass), and

$$\mathcal{R}_{0pv} = \frac{\beta_{1p}\beta_{p1} P^* V_1^*}{\rho_1 (r + \delta + \alpha)} + \frac{\beta_{2p}\beta_{p2} P^* V_2^*}{\rho_2 (r + \delta + \alpha)} + \frac{\beta_{3p}\beta_{p3} P^* V_3^*}{\rho_3 (r + \delta + \alpha)},$$

represent a horizontal transmission (through vectors). When there is no vertical transmission, i.e., $\mathcal{R}_{0v} = 0$, the reproduction number reduces to the geometric mean of the number of new infections in plants from one infected vector.

Remark 2. *Some remarks are in order regarding the interpretation of $\mathcal{R}_{0pv}$. First we rewrite $\mathcal{R}_{0pv}$ in equation (3.7) in the form $\mathcal{R}_{0pv} = \mathcal{R}_{01} + \mathcal{R}_{02} + \mathcal{R}_{03}$, where*

$$\mathcal{R}_{01} = \frac{\beta_{1p}\beta_{p1}P^*V_1^*}{\rho_1(r+\delta+\alpha)}, \quad \mathcal{R}_{02} = \frac{\beta_{2p}\beta_{p2}P^*V_2^*}{\rho_2(r+\delta+\alpha)}, \quad \mathcal{R}_{03} = \frac{\beta_{3p}\beta_{p3}P^*V_3^*}{\rho_3(r+\delta+\alpha)}.$$

The threshold $\mathcal{R}_{01}$ is associated with the disease transmission by infected first-instars. In this threshold parameter, $\dfrac{\beta_{p1}P^*}{\rho_1}$ gives the threshold from infected grapevine to healthy plants, and $\dfrac{\beta_{1p}V_1^*}{r+\alpha+\delta}$ gives threshold for the infection of first-instars by diseased plants. Similarly, $\mathcal{R}_{02}$ and $\mathcal{R}_{03}$ are the threshold parameters associated with the second- and third-instars respectively. It is clear from these threshold values that increasing roguing will decrease the value of $\mathcal{R}_0$. In addition, the use of insecticides, akin to increasing the natural mortality, has the same epidemiological result of reducing $\mathcal{R}_0$.

Following [27], and the derivation of the threshold parameter in (3.7), we deduce the following result,

Theorem 2. *If $\mathcal{R}_0 < 1$, the disease-free equilibrium E_{DFE} is locally asymptotically stable. If $\mathcal{R}_0 > 1$, the disease-free equilibrium is unstable.*

Several boundary equilibria exist for the model (3.1). These include the full-disease equilibrium (the case, $S_p = 0$) and cases where at least one of the vector compartments is disease-free, i.e., $I_i = 0$ for each $i = 1, 2, 3$.

We begin here by assuming $S_p = 0$, to get the full-disease equilibrium. This is the case when the whole crop is infected. The equilibrium is given by $E_{\text{FDE}} = (S_1^\circ, I_1^\circ, S_2^\circ, I_2^\circ, S_3^\circ, I_3^\circ, 0, I_p^\circ)^t$ where

$$S_1^\circ = \frac{V_1^*\rho_1}{\rho_1 + \beta_{p1}I_p^\circ}, \; I_1^\circ = \frac{V_1^*\beta_{p1}I_p^\circ}{\rho_1 + \beta_{p1}I_p^\circ}, \; S_2^\circ = \frac{V_2^*\rho_2}{\rho_2 + \beta_{p2}I_p^\circ},$$

$$I_2^\circ = \frac{V_2^*\beta_{p2}I_p^\circ}{\rho_2 + \beta_{p2}I_p^\circ}, \; S_3^\circ = \frac{V_3^*\rho_3}{\rho_3 + \beta_{p3}I_p^\circ}, \; I_3^\circ = \frac{V_3^*\beta_{p3}I_p^\circ}{\rho_3 + \beta_{p3}I_p^\circ},$$

with $I_p^\circ = \dfrac{r-(\alpha+\delta)}{m}$. Linearisation shows that E_{FDE} is locally asymptotically stable provided $r > \alpha + \delta$ and

$$(\alpha+\delta) - (I_1^\circ\beta_{1p} + I_2^\circ\beta_{2p} + I_3^\circ\beta_{3p}) < 0,$$

see Appendix A for the derivation of this condition. The first condition is related to the existence of the equilibrium, while the later condition comes from the linearisation process. It is not clear, however, how this condition can be expressed in terms of the basic reproduction number of the system, hence we will proceed numerically, see Section 5. In particular, Fig. 9 illustrates the existence and global stability of the full disease equilibrium E_{FDE} and the endemic equilibrium E_{EE} for $\mathcal{R}_0 > 1$. However, here we will give some insight into the existence and stability of this equilibrium by considering the reduced non-age-structure system in Section 4.

3.2 Co-existence equilibrium

In this section we assume $I_p \neq 0$. Setting the right hand side of the system (3.1) to zero, we have

$$\begin{aligned}
0 &= \Lambda - \lambda_1 S_1 - (\gamma_1 + \mu_1) S_1 + \omega I_1, \\
0 &= \lambda_1 S_1 - \rho_1 I_1, \\
0 &= \gamma_1 S_1 - \lambda_2 S_2 - (\gamma_2 + \mu_2) S_2 + \omega I_2 + \gamma_1 I_1, \\
0 &= \lambda_2 S_2 - \rho_2 I_2, \\
0 &= \gamma_2 S_2 - \lambda_3 S_3 + \omega I_3 - (\mu_3 + \gamma_3) S_3 + \gamma_2 I_2, \\
0 &= \lambda_3 S_3 - \rho_3 I_3, \\
0 &= r S_p - m P S_p - \lambda_p S_p, \\
0 &= r I_p - m P I_p + \lambda_p S_p - (\delta + \alpha) I_p,
\end{aligned} \tag{3.8}$$

where equation $(3.8)_2$ gives $S_1^* = \dfrac{\rho_1 I_1^*}{\beta_{p1} I_p^*}$, and substituting this into $(3.8)_1$, and after some manipulation, we find

$$I_1^* = \frac{\beta_{p1} V_1^* I_p^*}{\beta_{p1} I_p^* + \rho_1}.$$

Similarly, from equations $(3.8)_3$ - $(3.8)_6$, we get

$$I_2^* = \frac{\beta_{p2} V_2^* I_p^*}{\beta_{p2} I_p^* + \rho_2}, \quad I_3^* = \frac{\beta_{p3} V_3^* I_p^*}{\beta_{p3} I_p^* + \rho_3}.$$

With $(3.8)_7$ in mind, we can now see that

$$\begin{aligned}
\sum_{i=1}^{3} \beta_{ip} I_i^* =& \frac{\beta_{1p}\beta_{p1} V_1^* I_p^*}{\beta_{p1} I_p^* + \rho_1} + \frac{\beta_{2p}\beta_{p2} V_2^* I_p^*}{\beta_{p2} I_p^* + \rho_2} + \frac{\beta_{3p}\beta_{p3} V_3^* I_p^*}{\beta_{p3} I_p^* + \rho_3} \\
=& \frac{r + \alpha + \delta}{P^*} \left[\frac{\mathcal{R}_{01}\rho_1}{\beta_{p1} I_p^* + \rho_1} + \frac{\mathcal{R}_{02}\rho_2}{\beta_{p2} I_p^* + \rho_2} + \frac{\mathcal{R}_{03}\rho_3}{\beta_{p3} I_p^* + \rho_3} \right] I_p^*.
\end{aligned}$$

Equation $(3.8)_7$ can be solved for S_p^* to get

$$S_p^* = \frac{1}{m} \left(r - m I_p^* - \frac{m(r + \alpha + \delta)}{r} \left[\frac{\mathcal{R}_{01}\rho_1}{\beta_{p1} I_p^* + \rho_1} + \frac{\mathcal{R}_{02}\rho_2}{\beta_{p2} I_p^* + \rho_2} + \frac{\mathcal{R}_{03}\rho_3}{\beta_{p3} I_p^* + \rho_3} \right] I_p^* \right), \tag{3.9}$$

and substituting equation (3.9) into $(3.8)_5$ we get a sixth order polynomial equation in I_p^* of the form

$$a_6 {I_p^*}^6 + a_5 {I_p^*}^5 + a_4 {I_p^*}^4 + a_3 {I_p^*}^3 + a_2 {I_p^*}^2 + a_1 I_p^* + a_0 = 0, \tag{3.10}$$

where the coefficients, $a_0, \ldots, a_6$, are given in Appendix B. Clearly, when $\mathcal{R}_{0pv} \leq 1$, all coefficients are negative, suggesting there are no positive roots for $I_p^* \neq 0$. On the other hand, if $\mathcal{R}_{0pv} > 1$ (i.e., $\mathcal{R}_0 > 1$), a_0 is strictly positive while a_6 is strictly negative. Using Descarte's rule of signs, this suggests the existence of at least 1 positive root endemic equilibrium $E_{\text{EE}} = (S_1^*, I_1^*, S_2^*, I_2^*, S_3^*, I_3^*, S_p^*, I_p^*)^t$ for $\mathcal{R}_0 > 1$. In Fig. 9 illustrate the global stability of the endemic equilibrium E_{EE} when $\mathcal{R}_0 > 1$.

4 Contribution of age-structure

In this section we will qualitatively investigate the dynamics of model (3.1) in the absence of age-structure. To this end, we assume $S_v = S_1+S_2+S_3$, $I_v = I_1+I_2+I_3$, $\beta_{pv} = \beta_{p1} = \beta_{p2} = \beta_{p3}$, $\beta_{vp} = \beta_{1p} = \beta_{2p} = \beta_{3p}$, $\mu_v = \mu_1 = \mu_2 = \mu_3$, and $\gamma_v = \gamma_3$ with $\gamma_1 = \gamma_2 = 0$. The latter condition emphasises that maturation refers to development into adulthood since all instar stages are considered as a single stage. The assumption here is that all compartments have the same transmission and natural mortality rates. The reduced model for the vector population is given by

$$\begin{aligned} \frac{dS_v}{dt} &= \Lambda - \beta_{pv} I_p S_v - (\gamma_v + \mu_v) S_v + \omega I_v, \\ \frac{dI_v}{dt} &= \beta_{pv} I_p S_v - (\gamma_v + \mu_v) I_v - \omega I_v, \end{aligned} \tag{4.1}$$

while the reduced model for the plant biomass is given by

$$\begin{aligned} \frac{dS_p}{dt} &= rS_p - mPS_p - \beta_{vp} I_v S_p, \\ \frac{dI_p}{dt} &= rI_p - mPI_p + \beta_{vp} I_v S_p - (\delta + \alpha) I_p. \end{aligned} \tag{4.2}$$

Under this setup, γ_v denotes the maturation rate into adulthood. Adding all the equations in (4.1), we get

$$\frac{dV_r}{dt} = \Lambda - (\gamma_v + \mu_v) V_r, \quad V_r(0) = V_0 \geq 0, \tag{4.3}$$

where $V_r = S_v + I_v$. Similarly, adding equations in (4.2), gives

$$\frac{dP_r}{dt} = rP_r - mP_r^2 - (\delta + \alpha) I_p \leq rP_r - mP_r^2, \quad P_r(0) = P_0 \geq 0, \tag{4.4}$$

where $P_r = S_p + I_p$. From (4.3) and (4.4) we deduce that $V_r(t) \leq V_r^* = \dfrac{\Lambda}{\gamma_v + \mu_v}$ and $P_r(t) \leq P_r^* = \dfrac{r}{m}$, respectively, when $t \to \infty$. Clearly the model is mathematically and biologically well posed in

$$\Omega_r = \left\{ (S_v, I_v, S_p, I_p) \in \mathbb{R}_+^4 : S_v + I_v \leq V_r^*, S_p + I_p \leq P_r^* \right\}. \tag{4.5}$$

The disease-free-vineyard equilibrium for model (4.1) and (4.2) is given by $E_{\text{DFE}}^r = (V_r^*, 0, P_r^*, 0)^t$ and the associated basic reproduction number is obtained using the next generation matrix approach. In particular, similar to the approach in Section 3.1, we only consider the equations where the infection progress, and define

$$\mathcal{F}(X) = \begin{pmatrix} \beta_{pv} I_p S_v \\ \beta_{vp} I_v S_p + rI_p \end{pmatrix}, \quad \text{and} \quad \mathcal{V}(X) = \begin{pmatrix} (\gamma_v + \mu_v + \omega) I_v \\ (\alpha + \delta) I_p + mPI_p \end{pmatrix}.$$

where $X = (I_v, I_p)^t$. The terms $\mathcal{F}(X)$ and $\mathcal{V}(X)$ distinguishes the rate of appearance and disappearance of infections respectively. The next generation matrix is given by NGM$=J_{\mathcal{F}} J_{\mathcal{V}}^{-1}$

where

$$J_{\mathcal{F}} = \begin{pmatrix} 0 & \beta_{pv} V_r^* \\ \beta_{vp} P_r^* & r \end{pmatrix},$$

and

$$J_{\mathcal{V}} = \begin{pmatrix} \gamma_v + \mu_v + \omega & 0 \\ 0 & r + \alpha + \delta \end{pmatrix}.$$

The basic reproduction number, $\mathcal{J}_0$, is defined as the spectral radius of NGM at the disease-free equilibrium. This gives

$$\mathcal{J}_0 = \frac{\mathcal{J}_{0v}}{2} + \sqrt{\frac{\mathcal{J}_{0v}^2}{4} + \mathcal{J}_{0pv}}, \tag{4.6}$$

where

$$\mathcal{J}_{0v} = \frac{r}{r + \alpha + \delta},$$

represents vertical transmission through the production of new plant biomass, and

$$\mathcal{J}_{0pv} = \frac{\beta_{pv}\beta_{vp} P_r^* V_r^*}{(r + \delta + \alpha)(\gamma_v + \mu_v + \omega)},$$

represent a horizontal transmission through vectors. Clearly, from the derivation of (4.6), the disease-free equilibrium for the reduced model is locally asymptotically stable provided $\mathcal{J}_0 < 1$.

Remark 3. *We will make a remark here regarding the interpretation of the threshold value in* (4.6). *We can write* $\mathcal{J}_{0vp} = \mathcal{J}_0^p \mathcal{J}_0^v$ *where* $\mathcal{J}_0^v = \dfrac{\beta_{vp} V_r^*}{r + \delta + \alpha}$ *and* $\mathcal{J}_0^p = \dfrac{\beta_{pv} P_r^*}{\gamma_v + \mu_v + \omega}$. *The term* $\mathcal{J}_0^v$ *gives the threshold from infected Pl. ficus to susceptible grapevine, while* $\mathcal{J}_0^p$ *gives the threshold value from infected grapevine to susceptible Pl. ficus.*

We can improve on the local stability result of the disease-free equilibrium and prove global stability. To do this, we follow the work of [29] and split the uninfected compartments $x = (S_v, S_p)^t$ from the infected compartments $y = (I_v, I_p)^t$, with $E_{\text{DFE}}^r = (x^*, \mathbf{0})^t$ and $x^* = (V_r^*, P_r^*)^t$, so that the system can be summarised as follows

$$\frac{dx}{dt} = f(x, y), \quad \frac{dy}{dt} = g(x, y),$$

where

$$f(x, y) = \begin{pmatrix} \Lambda - \beta_{pv} I_p S_v - (\gamma_v + \mu_v) S_v + \omega I_v \\ r S_p - m P S_p - \beta_{vp} I_v S_p \end{pmatrix}$$

and

$$g(x, y) = \begin{pmatrix} \beta_{pv} I_p S_v - (\gamma_v + \mu_v) I_v - \omega I_v \\ r I_p - m P I_p + \beta_{vp} I_v S_p - (\delta + \alpha) I_p \end{pmatrix}$$

such that $g(x, 0) = 0$. Using [29], we need to verify the following conditions to guarantee the global asymptotic stability of the disease-free equilibrium.

$\mathcal{H}_1$**:** For $\dfrac{dx}{dt} = f(x, 0)$, x^* is globally asymptotically stable,

$\mathcal{H}_2$**:** $g(x, y) = J_g(E_{\text{DFE}}^r) y - \hat{g}(x, y)$, $\hat{g}(x, y) \geq 0$ for $(x, y) \in \Omega$,

where $J_g(E^r_{\text{DFE}})$, the Jacobian of function of $g(x,y)$ at E^r_{DFE}, is a Metzler-matrix and Ω is the region defined in (3.4). Clearly, condition $\mathcal{H}_1$ is satisfied for the subsystem. In particular, we see that the last equation in the system is a Logistic equation for which P^*_r is globally asymptotically stable. To check $\mathcal{H}_2$, we write the Jacobian of $g(x,y)$ at x^*, given by

$$J_g(E^r_{\text{DFE}}) = \begin{pmatrix} -(\gamma_v+\mu_v+\omega) & \beta_{pv}V^*_r \\ \beta_{vp}P^*_r & -(\alpha+\delta) \end{pmatrix},$$

which is a Metzler-matrix (off diagonal elements are nonnegative), so that

$$g(x,y) = J_g(E^r_{\text{DFE}})y - (\beta_{pv}I_p(V^*_r - S_v), \beta_{vp}I_v(P^*_r - S_p))^t. \tag{4.7}$$

Following (4.5), clearly the last term on the right-hand-side of matrix equation (4.7), denoted in $\mathcal{H}_2$ as $\hat{g}(x,y)$, is nonnegative for all $(x,y) \in \Omega_r$. Therefore the disease-free equilibrium is globally asymptotically stable. We summarise the result as follows:

Theorem 3. *The equilibrium point $E^r_{DFE} = (x^*, 0)^t$ is globally asymptotically stable provided $\mathcal{J}_0 < 1$ and unstable for $\mathcal{J}_0 > 1$.*

4.1 Existence and stability of boundary and interior equilibria

Setting the right-hand-side of the system (4.1) and (4.2) to zero, (with $S_p = 0$) we get the following equilibrium, $E^r_{\text{FDE}} = (S^\circ_v, I^\circ_v, 0, I^\circ_p)^t$, (the full-disease equilibrium) where,

$$S^\circ_v = \frac{(\gamma_v+\mu_v+\omega)V^*_r}{(\gamma_v+\mu_v+\omega)+\beta_{pv}I^\circ_p},\ I^\circ_v = \frac{\beta_{pv}I^\circ_pV^*_r}{(\gamma_v+\mu_v+\omega)+\beta_{pv}I^\circ_p},\ I^\circ_p = \frac{r-(\alpha+\delta)}{m}.$$

On the other hand, if $S_p \neq 0$ (and $I_p \neq 0$), we have the endemic equilibrium, $E^r_{\text{EE}} = (S^*_v, I^*_v, S^*_p, I^*_p)$, where S^*_v satisfies the quadratic equation

$$a_2S^{*2}_v + a_1S^*_v + a_0 = 0, \tag{4.8}$$

with the coefficients satisfying

$$a_2 = \frac{\beta_{pv}}{\beta_{vp}}(\gamma_v+\mu_v),\ a_1 = \frac{\beta_{pv}}{\beta_{vp}}[r(\gamma_v+\mu_v) - \Lambda\beta_{vp}],\ a_0 = -\frac{m}{\beta_{vp}}(\gamma_v+\mu_v)(\alpha+\delta)(\gamma_v+\mu_v+\omega_v).$$

Clearly, $a_2 > 0$, $a_0 < 0$ and the discriminant of equation (4.8) is positive. Using Descartes' rule of signs, a unique endemic equilibrium exists and is given by $S^*_v = (-a_1 + \sqrt{\Delta})/(2a_2)$. Furthermore, we have

$$I^*_v = \frac{\Lambda-(\gamma_v+\mu_v)S^*_v}{(\gamma_v+\mu_v)},\ S^*_p = \frac{(\gamma_v+\mu_v+\omega)}{\beta_{vp}\beta_{pv}S^*_v}((\alpha+\delta)-\beta_{vp}I^*_v),\ I^*_p = \frac{(\gamma_v+\mu_v+\omega)I^*_v}{\beta_{vp}S^*_v}.$$

It is clear that E^r_{EE} exists provided

$$(\alpha+\delta) - \beta_{vp}I^*_v > 0. \tag{4.9}$$

Proposition 1. *The model system* (4.1) *and* (4.2) *admits the following non-zero equilibria:* (*a*) *the disease-free equilibrium* E^r_{DFE}, (*b*) *the full-disease equilibrium,* E^r_{FDE}, *provided* $r > \alpha + \delta$, *and* (*c*) *the endemic equilibrium* E^r_{EE} *provided* $(\alpha + \delta) - \beta_{vp} I^*_v > 0$.

We summarise the stability of the equilibria in Proposition 1 in the following result.

Theorem 4. *Consider the system* (4.1) *and* (4.2)*:*

(a) Assuming $\mathcal{J}_0 < 1$, *then* E^r_{DFE} *is globally asymptotically stable and unstable for* $\mathcal{J}_0 > 1$.

(b) Assuming $\mathcal{J}_{0pv} > 1$ *and* $r > \alpha + \delta$, *then* E^r_{FDE} *exists and is locally asymptotically stable.*

Proof. The proof of (a) follows from the derivation of (4.6). The reader can see, for example [27] or Section 3.1, for further details.

To prove (b), we consider the following Jacobian of the system (4.1) and (4.2), evaluated at E_{FDE}, i.e.,

$$J(E_{\text{FDE}}) = \begin{pmatrix} -\beta_{vp} I^\circ_p - (\gamma_v + \mu_v) & \omega & 0 & -\beta_{pv} S^\circ_v \\ \beta_{pv} I^\circ_p & -(\gamma_v + \mu_v + \omega) & 0 & \beta_{pv} S^\circ_v \\ 0 & 0 & r - m I^\circ_p - \beta_{vp} I^\circ_v & 0 \\ 0 & 0 & \beta_{vp} I^\circ_v - m I^\circ_p & r - 2m I^\circ_p - (\delta + \alpha) \end{pmatrix}. \tag{4.10}$$

We expand in terms of the third row and find the first eigenvalue

$$\lambda_1 = r - m I^\circ_p - \beta_{vp} I^\circ_v = r - m \left(\frac{r - (\alpha + \delta)}{m} \right) - \beta_{vp} I^\circ_v = (\alpha + \delta) - \beta_{vp} I^\circ_v.$$

For local stability, we require that $\lambda_1 < 0$, and this is equivalent to $(\alpha + \delta) - \beta_{vp} I^\circ_v < 0$, or on further simplification

$$\mathcal{J}_{0pv} > 1 + \mathcal{J}^p_0 + \frac{\alpha + \delta}{r - (\alpha + \delta)} > 1, \tag{4.11}$$

where $\mathcal{J}^p_0$ is given in Remark 3. Next, expanding over the third row of the remaining matrix, we have

$$\lambda_2 = r - 2m I^\circ_p - (\delta + \alpha) = r - 2m \left(\frac{r - (\alpha + \delta)}{m} \right) - (\delta + \alpha) = (\delta + \alpha) - r < 0$$

to be the second eigenvalue. The remaining eigenvalues are found from the following reduced matrix

$$\begin{pmatrix} -\beta_{vp} I^\circ_p - (\gamma_v + \mu_v) & \omega \\ \beta_{pv} I^\circ_p & -(\gamma_v + \mu_v + \omega) \end{pmatrix} \tag{4.12}$$

whose trace is clearly negative, and the determinant is positive. Hence the full-disease equilibrium point is locally asymptotically stable provided condition (4.11) is satisfied, otherwise it is unstable. □

The condition in (4.11) shows that if $\mathcal{J}_0$ is sufficiently large enough, the whole crop will be infected. When $\mathcal{J}_0 > 1$, the model (4.1) and (4.2) has at least one endemic equilibrium which is locally asymptotically stable. We proceed using the Centre Manifold theory (see for example

[27, 30]), to show the local stability of the endemic equilibrium. Given that E^r_{DFE} is globally asymptotically stable, we can rule out the possibility of backward bifurcation in the model. Hence we state the following result (see Theorem 5) whose proof is provided in Appendix C.

Theorem 5. *The model* (4.1) *and* (4.2) *has at least one endemic equilibrium point which is locally asymptotically stable.*

Remark 4. *In summary, from the analysis of the age-structured model and the reduced model (without age-structure), we see similar qualitative properties in terms of equilibria and their asymptotic behavior. Both models have a unique disease-free equilibrium which is globally asymptotically stable for the threshold parameter less than unit. It is apparent that adding the age-structure does not alter the qualitative properties of the model. To investigate the quantitative properties of the models, we will proceed numerically in Section 5.*

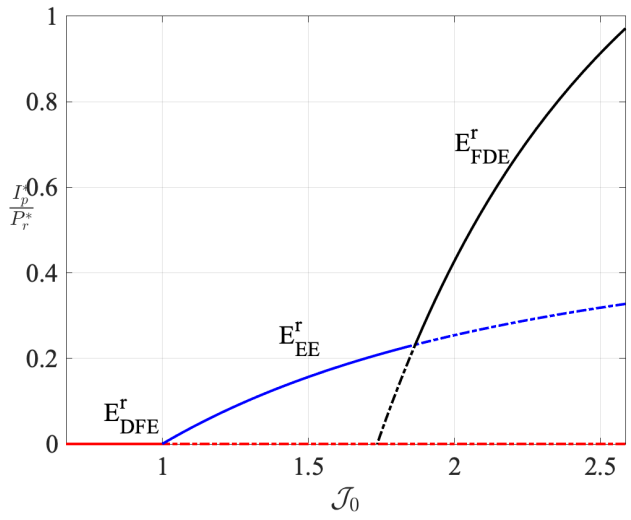

Figure 5: Bifurcation diagram of the model (4.1) and (4.2) showing the stable trajectory (solid line) and the unstable trajectory (broken line).

We support the qualitative analysis of the age-structured and reduced models through numerical simulations, see Figs. 5, 6, 7, 8 and 9. In particular, Fig. 5 confirms that if $\mathcal{J}_0$ is sufficiently large, the whole crop will be infected. Fig. 6 and Fig. 7 support results in Theorem 4. In addition, considering the full model, numerical results in Fig. 8 and Fig. 9 support the existence and stability of the model equilibria. We also notice from Fig. 5 that if $\mathcal{J}_0$ is sufficiently very large, then the whole crop will be infected.

It is clear from the numerical simulations that if only infected plants are used for new biomass, the whole crop will be infected. Roguing remains the most effective way to control the spread of GLRv-3 virus.

5 Numerical results

In this section we provide numerical results for the full GLRv-3 transmission model summarised in equations (3.1). In particular, the equations are solved using `MatLab`'s ode-solver with the

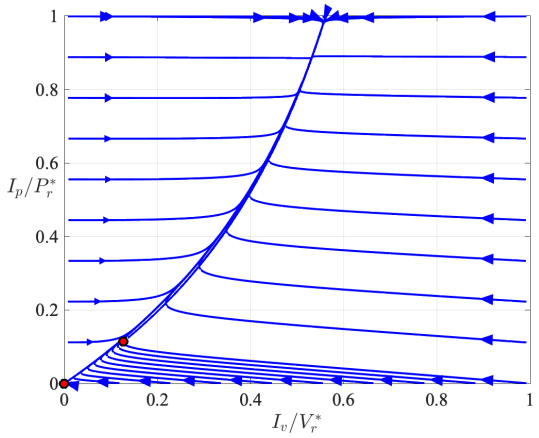

(a) Stability for $\mathcal{J}_0 > 1$.

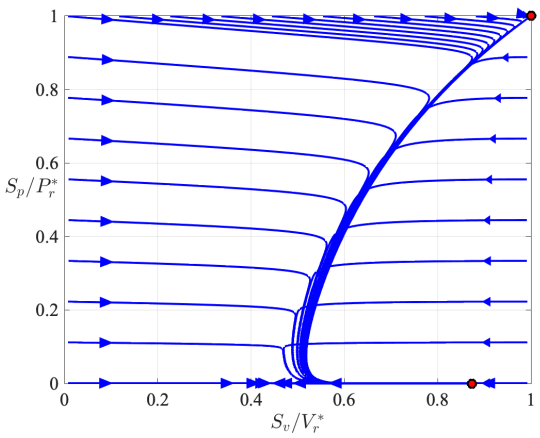

(b) Stability for $\mathcal{J}_0 > 1$.

Figure 6: Illustration of Theorem 4(b) for the reduced model (4.1) with (4.2) for $\mathcal{J}_0 = 3.293$. We take $\beta_{vp} = 0.0004$.

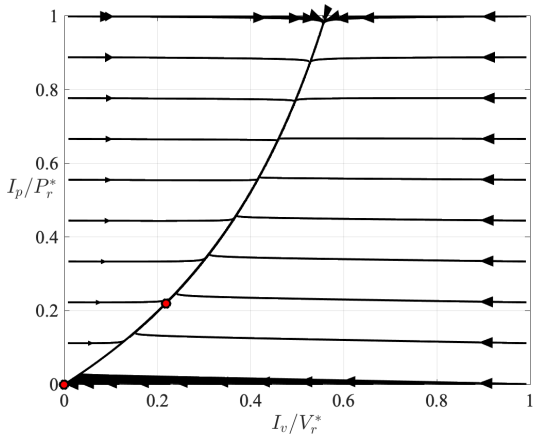

(a) Stability for $\mathcal{J}_0 > 1$.

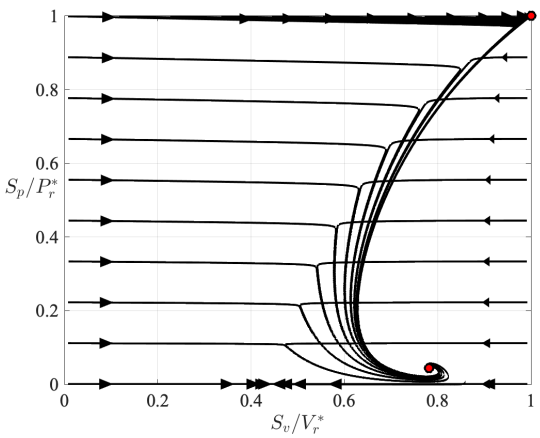

(b) Stability for $\mathcal{J}_0 > 1$.

Figure 7: Illustration of Theorem 5 for the reduced model (4.1) and (4.2) with $\mathcal{J}_0 = 1.796$ when condition (4.9) is satisfied. All trajectories converge to E_{EE}^r.

solver's `Reltol` and `AbsTol` set so that the simulations converge. Unless stated otherwise under the figure caption, the parameters are chosen as given in Table 2. In addition to parameters in Table 2, we also have $\beta_{vp} = \beta_{pv} = 0.0013$, $\mu_v = 0.0655$, and $\gamma_v = 0.179$ for the reduced model.

5.1 Local sensitivity analysis

We first perform a sensitivity analysis on the basic reproduction number, $\mathcal{R}_0$, in order to capture how the ratio responds to changes in the parameters, furthermore, gain understanding into the disease control strategy and the transmission dynamics described of model (3.1). The changes in or sensitivity of $\mathcal{R}_0$ with respect to a parameter q is mathematically given by $\varphi_{\mathcal{R}_0}^q = \dfrac{\partial \mathcal{R}_0}{\partial q}$. The concept of sensitivity only looks at local computation while all parameters are kept constant.

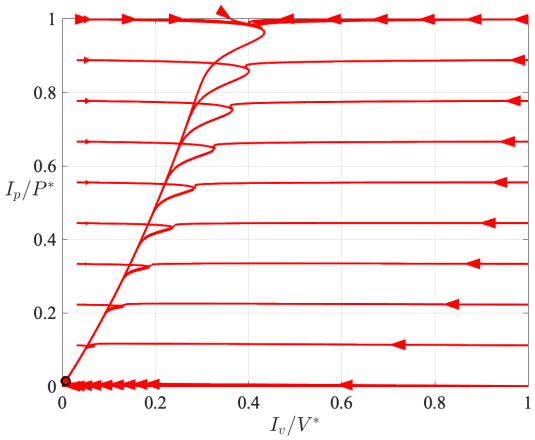

Figure 8: Illustration of Theorem 3 for the full model (3.1) for $\mathcal{R}_0 = 0.8510$.

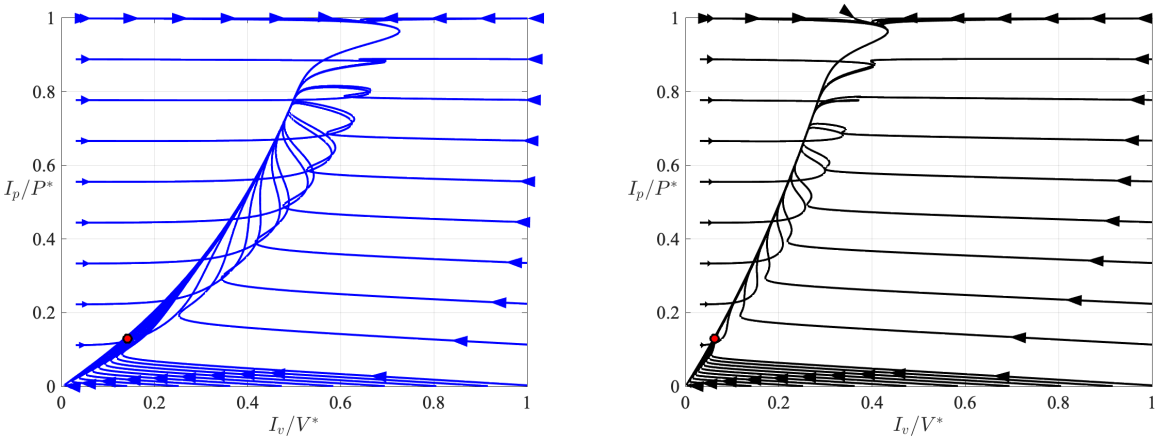

(a) Stability for $\mathcal{R}_0 = 2.890$.

(b) Stability for $\mathcal{R}_0 = 1.938$.

Figure 9: Illustration of the stability of the equilibrium points for $\mathcal{R}_0 > 1$. On the left, all trajectories converge to E_{FDE}, and on the right, all trajectories converge to E_{EE}.

That is, sensitivity does not consider the simultaneous variation of all parameters. Thus, we will make use of the percentage change in $\mathcal{R}_0$ with respect to the percentage change in the parameter q, referred to as elasticity or sensitivity index. Particularly, we calaculate $\varepsilon^q_{\mathcal{R}_0} = \dfrac{\partial \mathcal{R}_0}{\partial q}\dfrac{q}{\mathcal{R}_0}$. The elasticity of $\mathcal{R}_0$ with respect to q is negative if $\mathcal{R}_0$ is decreasing with respect to q, and positive if $\mathcal{R}_0$ is increasing with respect to q. The local sensitivity analysis on the basic reproduction ratio leads to the numerical values shown in Table 2. The most sensitive parameters are Λ, r and m. However, among the parameters that can be used to control the spread of the disease, we have the contact rates β_{pi} and β_{ip}, for $i = 1, 2, 3$. This can be implemented by, for example, the use of nets.

Parameters	Baseline value	Sensitivity index
Λ	29	0.5000
ω	0.33	-0.3680
$\mu_1/\mu_2/\mu_3$	0.00003/0.000027/0.00001	-0.0000956/-0.0001028/-0.00001200
$\gamma_1/\gamma_2/\gamma_3$	0.179/0.0921/0.0613	-0.2716/-0.3503/-0.009940
$\beta_{p1}/\beta_{p2}/\beta_{p3}$	0.0008/0.0004/0.0001	0.2010/0.2355/0.06350
$\beta_{1p}/\beta_{2p}/\beta_{3p}$	0.0013/0.0013/0.0013	0.2010/0.2355/0.06350
r	0.0035	-0.5000
m	0.000003	0.5000
δ	0.003	-0.4839
α	0.0001	-0.01613

Table 2: Baseline parameter values for model (3.1). The baseline parameter values give $\mathcal{R}_0 = 2.8904$.

5.2 Assessing the effectiveness of control measures

To assess the effect of roguing on the control of GLRv-3 transmission, we perform simulations where δ is varied in the range $[0, 1]$. For the purpose of comparison between the age-structured model and the reduced model, the parameters for the reduced model are selected by taking the mean average for μ_i, γ_i, β_{pi} and β_{ip}, to get values for $\mu_v, \gamma_v, \beta_{pv}$ and β_{vp} respectively with $i = 1, 2, 3$. The simulations are provided in Figs. 11 and 10. In Fig. 10 we assume sanitary measures regarding the use of certified clean plants are in place. This is the case when no vertical transmission is included in the model. Clearly less effort (roguing) is required to control the virus compared to the case where less strict sanitary measures are in place, see Fig. 11.

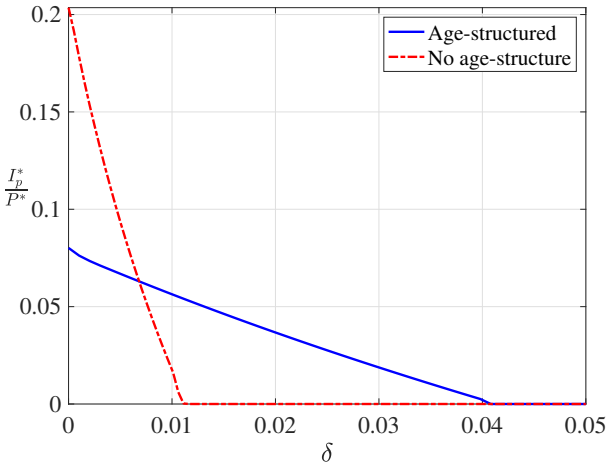

Figure 10: Bifurcation with respect to δ for the models assessing the effect of roguing, δ on the control of GLRv-3 transmission when only clean plants are using for replanting.

On the other hand, we observe that, for the selected parameter values, more effort in terms of roguing is required to control the virus when age-structured is taken into account compared to the case where no age-structure is considered. This is particularly important to avoid premature

end in implementing control strategies.

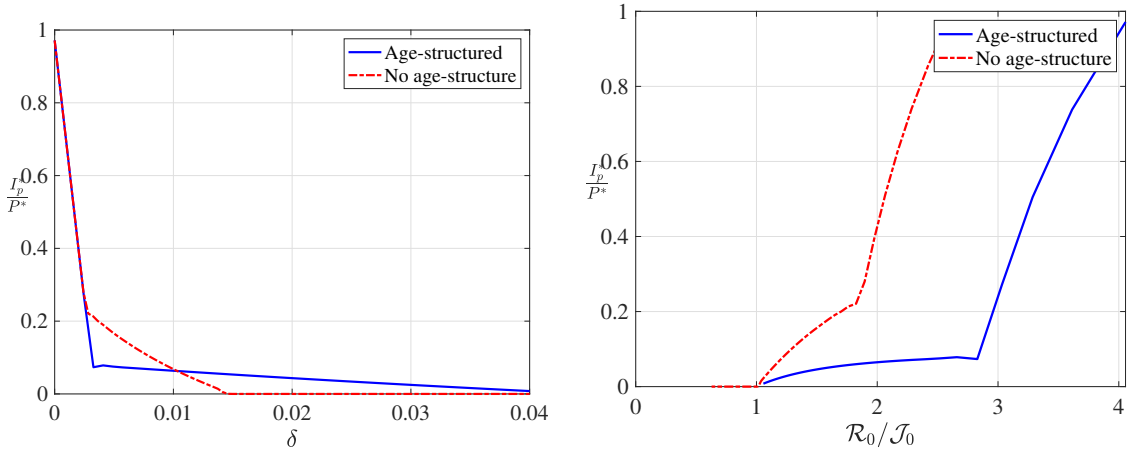

(a) Bifurcation with respect to δ. (b) Bifurcation with respect to $\mathcal{R}_0$.

Figure 11: Bifurcation diagram of the models assessing the effect of roguing, δ on the control of GLRv-3 transmission when both infected and clean plants are selected for replanting.

6 Conclusions

In this paper, we presented an age-structured mathematical model for the transmission of GLRaV-3 by *Pl. ficus* in grapevines. A threshold value, the basic reproduction ratio, $\mathcal{R}_0$, was computed using the next generation matrix approach to investigate the asymptotic properties of the model. The proposed model is rather generic and could be applied to other plant-vector-virus interactions, specifically those separated by life stages of vector. Better insight into the dynamics of the model we analysed using a reduced model where only the combined vector population is taken into account. Numerical solutions of the system under different control strategies were presented in order to examine their contribution to disease control. The importance of roguing as a control measure was presented and results were in support with the literature that roguing was an effective and economic control strategy [24]. The results in Figs. 11 and 10 reiterates the importance of clean healthy plants in varieties that do not show symptoms. Based on the value of $\mathcal{R}_0$, the use of insecticides as a control measure can also be an effective way of controlling the virus by increasing the vector mortality. This strategy has been used successfully in, for example, citrus growing regions, see [31] for a review of these control measures. However, it has been reported that the use of pesticides can repel the pests causing a rapid movement in (non-treated) parts of the crops, and thus causing greater spreading of the diseases [32]. Future work will include the global sensitivity analysis and modeling the effects of temperature of the dynamics.

Acknowledgements

The author acknowledges the support of South African DSI/NRF SARChI Chair on Mathematical Models and Methods in Bioengineering and Biosciences (M^3B^2) of the University of

Pretoria. The authors are grateful to the anonymous reviewers and the Handling Editor for their excellent suggestions and comments that have greatly contributed to improve the manuscript.

References

[1] S.T. Endeshaw, P. Sabbatini, G. Romanazzi, A. Schilder, and D. Neri. Effects of Grapevine leafroll associated virus 3 infection on growth, leaf gas exchange, yield and basic fruit chemistry of vitis vinifera l. cv. cabernet franc. *Scientia Horticulturae*, 170:228–236, 05 2014.

[2] H.J. Maree, R.P.P. Almeida, R. Bester, K.M. Chooi, D. Cohen, V.V. Dolja, M.F. Fuchs, D.A. Golino, A.E.C. Jooste, G.P. Martelli, et al. Grapevine leafroll-associated virus 3. *Frontiers in Microbiology*, 4:82, 2013.

[3] R.A. Naidu, S. O'Neil, and D. Walsh. Grapevine leafroll disease. WSU extension bulletin eb2027e. 20pp, 2008.

[4] G. Pietersen. Spread of Grapevine leafroll disease in South Africa difficult but not insurmountable problem. *Technical Yearbook 2004/5*, 2004.

[5] R. Almeida, K. Daane, V. Bell, G.K. Blaisdell, M. Cooper, E. Herrbach, and G. Pietersen. Ecology and management of Grapevine leafroll disease. *Frontiers in Microbiology*, 4:94, 2013.

[6] K. Krüger and N. Douglas-Smit. Grapevine leafroll-associated virus 3 (GLRaV-3) transmission by three soft scale insect species (hemiptera: Coccidae) with notes on their biology. *African Entomology*, 21(1):1–8, 2013.

[7] N. Mahfoudhi, M. Digiaro, and M.H. Dhouibi. Transmission of Grapevine leafroll viruses by *Planococcus ficus* (hemiptera: Pseudococcidae) and ceroplastes rusci (hemiptera: Coccidae). *Plant Disease*, 93(10):999–1002, 2009.

[8] G. Belli, A. Fortusini, P. Casati, L. Belli, P.A. Bianco, and S. Prati. Transmission of a grapevine leafroll associated closterovirus by the scale insect pulvinaria vitis l. *Rivista di Patologia Vegetale*, 4(3):105–108, 1994.

[9] K.M. Daane, R.P.P. Almeida, V.A. Bell, J.T.S. Walker, M. Botton, M. Fallahzadeh, M. Mani, J.L. Miano, R. Sforza, V.M. Walton, et al. Biology and management of mealybugs in vineyards. In *Arthropod Management in Vineyards:*, pages 271–307. Springer, 2012.

[10] V.M. Walton and K.L. Pringle. Vine mealybug, *Planococcus ficus* (signoret)(hemiptera: Pseudococcidae), a key pest in South African vineyards. A review. 2004.

[11] N. Douglas and K. Krüger. Transmission efficiency of Grapevine leafroll-associated virus 3 (GLRaV-3) by the mealybugs *Planococcus ficus* and *Pseudococcus* longispinus (Hemiptera: Pseudococcidae). *European Journal of Plant Pathology*, 122(2):207–212, 2008.

[12] G. De Lotto. Notes on the vine mealybug (homoptera: Coccoidea: Pseudococcidae). *Journal of the Entomological Society of Southern Africa*, 38(2):125–130, 1975.

[13] F. Brauer. Mathematical Epidemiology: Past, present, and future. *Infectious Disease Modelling*, 2(2):113–127, 2017.

[14] K. Krüger, D.L. Saccaggi, M. Van der Merwe, and G.G.F. Kasdorf. Transmission of Grapevine leafroll-associated virus 3 (GLRaV-3): acquisition, inoculation and retention by the mealybugs *Planococcus ficus* and pseudococcus longispinus (hemiptera: Pseudococcidae). *South African Journal of Enology and Viticulture*, 36(2):223–230, 2015.

[15] C.-W. Tsai, J. Chau, L. Fernandez, D. Bosco, K.M. Daane, and R.P.P. Almeida. Transmission of Grapevine leafroll-associated virus 3 by the vine mealybug (*Planococcus ficus*). *Phytopathology*, 98(10):1093–1098, 2008.

[16] G. Pietersen, N. Spreeth, T. Oosthuizen, A. van Rensburg, M. van Rensburg, D. Lottering, N. Rossouw, and D. Tooth. Control of Grapevine leafroll disease spread at a commercial wine estate in South Africa: a case study. *American Journal of Enology and Viticulture*, 64(2):296–305, 2013.

[17] K. Holm. *Construction of a cDNA library for the vine mealybug,* Planococcus ficus *(Signoret).* PhD thesis, Stellenbosch: Stellenbosch University, 2008.

[18] G. Pietersen and H. Walsh. Development of a lamp technique for control of Grapevine leafroll associated virus type 3 (GLRaV-3) in infected white cultivar vines by roguing. *ICVG 201*, 2012.

[19] M. Chapwanya and Y. Dumont. Application of mathematical epidemiology to crop vector-borne diseases: The cassava mosaic virus disease case. In *Teboh-Ewungkem M.I., Ngwa G.A. (eds). Infectious diseases and our Planet Earth. Mathematics of the Planet Earth*, volume 7, pages 57–95. Springer, 2021.

[20] Dimitris C Kontodimas, Panagiotis A Eliopoulos, George J Stathas, and Leonidas P Economou. Comparative temperature-dependent development of nephus includens (kirsch) and nephus bisignatus (boheman)(coleoptera: Coccinellidae) preying on planococcus citri (risso)(homoptera: Pseudococcidae): evaluation of a linear and various nonlinear models using specific criteria. *Environmental Entomology*, 33(1):1–11, 2004.

[21] V.M. Walton. *Development of an integrated pest management system for vine mealybug,* Planococcus ficus *(Signoret), in vineyards in the Western Cape Province, South Africa.* PhD thesis, Stellenbosch: Stellenbosch University, 2003.

[22] K. Varikou, A. Birouraki, N. Bagis, and D.C. Kontodimas. Effect of temperature on the development and longevity of *Planococcus ficus* (hemiptera: Pseudococcidae). *Annals of the Entomological Society of America*, 103(6):943–948, 2010.

[23] Harsimran Kaur Gill, Gaurav Goyal, and Jennifer Gillett-Kaufman. Citrus mealybug Planococcus citri (risso)(insecta: Hemiptera: Pseudococcidae). *EDIS*, 2012(9), 2012.

[24] Stephen Hesler, Rosemary Cox, Greg Loeb, and Marc Fuchs. Vineyard trial demonstrates effectiveness of roguing and replanting to curtail the spread of grapevine leafroll disease. *Research Focus 2021-4: Cornell Viticulture and Enology*, 2021-4, 2021.

[25] E.A. Coddington and N. Levinson. *Theory of ordinary differential equations*. Tata McGraw-Hill Education, 1955.

[26] F. Brauer, C. Castillo-Chavez, and Z. Feng. *Mathematical models in epidemiology*. Springer, 2019.

[27] P. Van den Driessche and J. Watmough. Reproduction numbers and sub-threshold endemic equilibria for compartmental models of disease transmission. *Mathematical Biosciences*, 180(1-2):29–48, 2002.

[28] O. Diekmann, J.A.P. Heesterbeek, and Michael G. Roberts. The construction of next-generation matrices for compartmental epidemic models. *Journal of the Royal Society Interface*, 7(47):873–885, 2010.

[29] C. Castillo-Chavez, F. Zhilan, and W. Huang. On the computation of $\mathcal{R}_0$ and its role on global stability. *In: Castillo-Chavez, C., Blower, S., Van der Driessche, P., Kirschner, D., Yakubu, A.A. (eds.) Mathematical Approaches for Emerging and Reemerging Infectious Diseases: An Introduction*, pages 229–250, Springer, New York 1998.

[30] C. Castillo-Chavez and B. Song. Dynamical models of tuberculosis and their applications. *Mathematical Biosciences & Engineering*, 1(2):361, 2004.

[31] Karen Manja and Mirella Aoun. The use of nets for tree fruit crops and their impact on the production: A review. *Scientia Horticulturae*, 246:110–122, 2019.

[32] Michael Chapwanya and Yves Dumont. On crop vector-borne diseases. impact of virus lifespan and contact rate on the traveling-wave speed of infective fronts. *Ecological Complexity*, 34:119–133, 2018.

Appendix

A Stability of $E_{\mathbf{FDE}}$

We investigate the local stability of the full-disease equilibrium by computing the Jacobian matrix at E_{FDE}, i.e., $J(E_{\text{FDE}})$ given by

$$\begin{pmatrix} -I_p^\circ\beta_{p1} - a_1 & \omega & 0 & 0 & 0 & 0 & 0 & -\beta_{p1}S_1^\circ \\ I_p^\circ\beta_{p1} & -a_1 - \omega & 0 & 0 & 0 & 0 & 0 & \beta_{p1}S_1^\circ \\ \gamma_1 & \gamma_1 & -I_p^\circ\beta_{p2} - a_2 & \omega & 0 & 0 & 0 & -\beta_{p2}S_2^\circ \\ 0 & 0 & -I_p^\circ\beta_{p2} & -a_2 - \omega & 0 & 0 & 0 & \beta_{p2}S_2^\circ \\ 0 & 0 & \gamma_2 & \gamma_2 & -I_p^\circ\beta_{p3} - a_3 & \omega & 0 & -\beta_{p3}S_3^\circ \\ 0 & 0 & 0 & 0 & I_p^\circ\beta_{p3} & -a_3 - \omega & 0 & \beta_{p3}S_3^\circ \\ 0 & 0 & 0 & 0 & 0 & 0 & -k_1 & 0 \\ 0 & 0 & 0 & 0 & 0 & 0 & k_2 & (\alpha+\delta) - r \end{pmatrix},$$

where $k_1 = (I_1^\circ\beta_{1p} + I_2^\circ\beta_{2p} + I_3^\circ\beta_{3p}) - (\alpha+\delta)$ and $k_2 = (I_1^\circ\beta_{1p} + I_2^\circ\beta_{2p} + I_3^\circ\beta_{3p}) - (r - (\alpha+\delta))$. For convenience, we have set $a_i = \gamma_i + \mu_i$, $i = 1, 2, 3$. Expanding along the seventh row, we have the first eigenvalue given by $-k_1$, i.e.,

$$\lambda_1 = -k_1 = (\alpha+\delta) - (I_1^\circ\beta_{1p} + I_2^\circ\beta_{2p} + I_3^\circ\beta_{3p}).$$

Next, we expand along the last row of the reduced matrix, we have the second eigenvalue given by $\lambda_2 = -(\alpha+\delta)$. The remaining eigenvalues are found from the matrix

$$\begin{pmatrix} -I_p^\circ\beta_{p1} - a_1 & \omega & 0 & 0 & 0 & 0 \\ I_p^\circ\beta_{p1} & -a_1 - \omega & 0 & 0 & 0 & 0 \\ \gamma_1 & \gamma_1 & -I_p^\circ\beta_{p2} - a_2 & \omega & 0 & 0 \\ 0 & 0 & -I_p^\circ\beta_{p2} & -a_2 - \omega & 0 & 0 \\ 0 & 0 & \gamma_2 & \gamma_2 & -I_p^\circ\beta_{p3} - a_3 & \omega \\ 0 & 0 & 0 & 0 & I_p^\circ\beta_{p3} & -a_3 - \omega \end{pmatrix}.$$

A straightforward manipulation gives the following eigenvalues $\lambda_3 = -a_1,\ \lambda_4 = -a_2,\ \lambda_5 = -a_3,$

$$\lambda_6 = -(\beta_{p1}I_p^\circ + a_1 + \omega),\ \lambda_7 = -(\beta_{p2}I_p^\circ + a_2 + \omega),\ \lambda_8 = -(\beta_{p3}I_p^\circ + a_3 + \omega).$$

Clearly the local stability of E_{FDE} is dependent on the sign of λ_1 in addition to the conditions for existence of the equilibrium point.

B Coefficients for equation (3.10)

The coefficients for polynomial (3.10) are given by

$$
\begin{aligned}
a_6 =& -amr(1-m)\beta_{p1}\beta_{p2}^2\beta_{p3}^2\mathcal{R}_{01} - bmr(1-m)\beta_{p1}^2\beta_{p2}\beta_{p3}^2\mathcal{R}_{02} - cmr(1-m)\beta_{p1}^2\beta_{p2}^2\beta_{p3}\mathcal{R}_{03}\\
&-r^2\beta_{p1}^2\beta_{p2}^2\beta_{p3}^2,\\
a_5 =& cr^2[\mathcal{R}_{03}-2]\beta_{p1}^2\beta_{p2}^2\beta_{p3} - \rho_3^2 m\mathcal{R}_{03}[m(\alpha+\delta)\mathcal{R}_{03}+r(1-m)]\beta_{p1}^2\beta_{p2}^2\\
&+br^2[\mathcal{R}_{02}-2]\beta_{p1}^2\beta_{p2}\beta_{p3}^2 - \rho_2^2 m\mathcal{R}_{02}[m(\alpha+\delta)\mathcal{R}_{02}+r(1-m)]\beta_{p1}^2\beta_{p3}^2\\
&+ar^2[\mathcal{R}_{01}-2]\beta_{p1}\beta_{p2}^2\beta_{p3}^2 - \rho_1^2 m\mathcal{R}_{01}[m(\alpha+\delta)\mathcal{R}_{01}+r(1-m)]\beta_{p2}^2\beta_{p3}^2\\
&-2bcm[m(\alpha+\delta)\mathcal{R}_{02}\mathcal{R}_{03}+r(1-m)(\mathcal{R}_{02}+\mathcal{R}_{03})]\beta_{1p}^2\beta_{p2}\beta_{p3}\\
&-2acm[m(\alpha+\delta)\mathcal{R}_{01}\mathcal{R}_{03}+r(1-m)(\mathcal{R}_{01}+\mathcal{R}_{03})]\beta_{p1}\beta_{p2}^2\beta_{p3}\\
&-2abm[m(\alpha+\delta)\mathcal{R}_{01}\mathcal{R}_{02}+r(1-m)(\mathcal{R}_{01}+\mathcal{R}_{02})]\beta_{p1}\beta_{p2}\beta_{p3}^2,
\end{aligned}
$$

$$
\begin{aligned}
a_4 =& 2bcr^2[(\mathcal{R}_{0pv}-1)-(\mathcal{R}_{01}+1)]\beta_{p1}^2\beta_{p2}\beta_{p3} + 2acr^2[(\mathcal{R}_{0pv}-1)-(\mathcal{R}_{02}+1)]\beta_{p1}\beta_{p2}^2\beta_{p3}\\
&+2abr^2[(\mathcal{R}_{0pv}-1)-(\mathcal{R}_{03}+1)]\beta_{p1}\beta_{p2}\beta_{p3}^2\\
&+\rho_1^2r^2(\mathcal{R}_{01}-1)\beta_{p2}^2\beta_{p3}^2 - \rho_1^2bm[2m(\alpha+\delta)\mathcal{R}_{01}(\mathcal{R}_{01}+\mathcal{R}_{02})+r(1-m)(\mathcal{R}_{01}+\mathcal{R}_{02})]\beta_{p2}\beta_{p3}^2\\
&+\rho_2^2r^2(\mathcal{R}_{02}-1)\beta_{p1}^2\beta_{p3}^2 - ab^2m[2m(\alpha+\beta)\mathcal{R}_{02}(\mathcal{R}_{01}+\mathcal{R}_{02})+r(1-m)(\mathcal{R}_{01}+\mathcal{R}_{02})]\beta_{p1}\beta_{p3}^2\\
&+\rho_3^2r^2(\mathcal{R}_{03}-1)\beta_{p1}^2\beta_{p2}^2 - bc^2m[2m(\alpha+\delta)\mathcal{R}_{03}(\mathcal{R}_{02}+\mathcal{R}_{03})+r(1-m)(\mathcal{R}_{02}+\mathcal{R}_{03})]\beta_{p1}^2\beta_{p2}\\
&-\rho_1^2cm[2m(\alpha+\delta)\mathcal{R}_{01}(\mathcal{R}_{01}+\mathcal{R}_{03})+r(1-m)(\mathcal{R}_{01}+\mathcal{R}_{03})]\beta_{p2}^2\beta_{p3}\\
&-\rho_2^2cm[2m(\alpha+\delta)\mathcal{R}_{02}(\mathcal{R}_{02}+\mathcal{R}_{03})+r(1-m)(\mathcal{R}_{02}+\mathcal{R}_{03})]\beta_{p1}^2\beta_{p3}\\
&-ac^2m[2m(\alpha+\delta)\mathcal{R}_{03}(\mathcal{R}_{01}+\mathcal{R}_{03})+r(1-m)(\mathcal{R}_{01}+\mathcal{R}_{03})]\beta_{p1}\beta_{p2}^2\\
&-4abcm[m(\alpha+\delta)(\mathcal{R}_{01}\mathcal{R}_{02}+\mathcal{R}_{01}\mathcal{R}_{03}+\mathcal{R}_{02}\mathcal{R}_{03})+r(1-m)\mathcal{R}_{0pv}]\beta_{p1}\beta_{p2}\beta_{p3},
\end{aligned}
$$

$$
\begin{aligned}
a_3 =& bc^2r^2[(\mathcal{R}_{0pv}-1)-(2\mathcal{R}_{01}+\mathcal{R}_{02})]\beta_{p2}\beta_{p1}^2 + \rho_2^2cr^2[(\mathcal{R}_{0pv}-1)-(2\mathcal{R}_{01}+\mathcal{R}_{03})]\beta_{p3}\beta_{p1}^2\\
&+\rho_1^2br^2[(\mathcal{R}_{0pv}-1)-(2\mathcal{R}_{03}+\mathcal{R}_{02})]\beta_{p3}^2\beta_{p2} + ac^2r^2[(\mathcal{R}_{0pv}-1)-(\mathcal{R}_{01}+2\mathcal{R}_{02})]\beta_{p2}^2\beta_{p1}\\
&+\rho_1^2cr^2[(\mathcal{R}_{0pv}-1)-(2\mathcal{R}_{02}+\mathcal{R}_{03})]\beta_{p2}^2\beta_{p3} + ab^2r^2[(\mathcal{R}_{0pv}-1)-(2\mathcal{R}_{03}+\mathcal{R}_{01})]\beta_{p3}^2\beta_{p1}\\
&-2abc^2m[m(\alpha+\delta)(2\mathcal{R}_{0pv}\mathcal{R}_{03}+\mathcal{R}_{01}\mathcal{R}_{02})+r(1-m)(\mathcal{R}_{0pv}+\mathcal{R}_{03})]\beta_{p2}\beta_{p1}\\
&-2ab^2cm[m(\alpha+\delta)(2\mathcal{R}_{0pv}\mathcal{R}_{02}+\mathcal{R}_{02}\mathcal{R}_{03})+r(1-m)(\mathcal{R}_{0pv}+\mathcal{R}_{02})]\beta_{p3}\beta_{p1}\\
&-2a^2bcm[m(\alpha+\delta)(2\mathcal{R}_{0pv}\mathcal{R}_{01}+\mathcal{R}_{02}\mathcal{R}_{03})+r(1-m)(\mathcal{R}_{0pv}+\mathcal{R}_{01})]\beta_{p3}\beta_{p2}\\
&-\rho_2^2c^2m(\mathcal{R}_{02}+\mathcal{R}_{03})[m(\alpha+\delta)(\mathcal{R}_{02}+\mathcal{R}_{03})+r(1-m)]\beta_{p1}^2\\
&-\rho_1^2c^2m(\mathcal{R}_{01}+\mathcal{R}_{03})[m(\alpha+\delta)(\mathcal{R}_{01}+\mathcal{R}_{03})+r(1-m)]\beta_{p2}^2\\
&-\rho_1^2b^2m(\mathcal{R}_{01}+\mathcal{R}_{02})[m(\alpha+\delta)(\mathcal{R}_{01}+\mathcal{R}_{02})+r(1-m)]\beta_{p3}^2 + 4abcr^2(\mathcal{R}_{0pv}-1)\beta_{p3}\beta_{p2}\beta_{p1},
\end{aligned}
$$

$$
\begin{aligned}
a_2 =&\rho_2^2c^2r^2[(\mathcal{R}_{0pv}-1)-\mathcal{R}_{01}]\beta_{p1}^2-ab^2c^2m[2(\alpha+\delta)m\mathcal{R}_{0pv}(\mathcal{R}_{02}+\mathcal{R}_{03})+r(1-m)(\mathcal{R}_{0pv}+(\mathcal{R}_{02}+\mathcal{R}_{03}))]\beta_{p1}\\
&+2abc^2r^2[2(\mathcal{R}_{0pv}-1)-(\mathcal{R}_{01}+\mathcal{R}_{02})]\beta_{p1}\beta_{p2}+2ab^2cr^2[2(\mathcal{R}_{0pv}-1)-(\mathcal{R}_{01}+\mathcal{R}_{03})]\beta_{p3}\beta_{p1}\\
&+\rho_1^2c^2r^2[(\mathcal{R}_{0pv}-1)-\mathcal{R}_{02}]\beta_{p2}^2-\rho_1^2bc^2m[2(\alpha+\beta)m\mathcal{R}_{0pv}(\mathcal{R}_{01}+\mathcal{R}_{03})+r(1-m)(\mathcal{R}_{0pv}+(\mathcal{R}_{01}+\mathcal{R}_{03}))]\beta_{p2}\\
&+2a^2bcr^2[2(\mathcal{R}_{0pv}-1)-(\mathcal{R}_{20}+\mathcal{R}_{03})]\beta_{p3}\beta_{p2}\\
&+\rho_1^2b^2r^2[(\mathcal{R}_{0pv}-1)-\mathcal{R}_{03}]\beta_{p3}^2-\rho_1^2b^2cm[2(\alpha+\delta)m\mathcal{R}_{0pv}(\mathcal{R}_{01}+\mathcal{R}_{02})+r(1-m)\mathcal{R}_{0pv}+(\mathcal{R}_{01}+\mathcal{R}_{02})]\beta_{p3},\\
a_1 =&ab^2c^2r^2[2(\mathcal{R}_{0pv}-1)-\mathcal{R}_{01}]\beta_{p1}+\rho_1^2bc^2r^2[2(\mathcal{R}_{0pv}-1)-\mathcal{R}_{02}]\beta_{p2}+\rho_1^2b^2cr^2[2(\mathcal{R}_{0pv}-1)-\mathcal{R}_{03}]\beta_{p3}\\
&-\rho_1^2b^2c^2\mathcal{R}_{0pv}[m(\alpha+\delta)\mathcal{R}_{0pv}+r(1-m)],\\
a_0 =&\rho_1^2b^2c^2r^2(\mathcal{R}_{0pv}-1).
\end{aligned}
$$

C Proof of Theorem 5

Proof. We will prove this result using the Centre Manifold theory [27, 30]. In particular, we check the stability of the system at $\mathcal{J}_0 = 1$ by finding the signs of a and b as stated in Theorem 4.1 of [30]. To this end, we set the following variables

$$x_1 = V_r^* - S_v,\ x_2 = I_v,\ x_3 = P_r^* - S_p,\ x_4 = I_p.$$

We also choose β_{pv} as the bifurcation parameter, which is given by $\phi = \dfrac{(\alpha+\delta)(\gamma_v+\mu_v+\omega)}{\beta_{vp}P_r^*V_r^*}$ at $\mathcal{J}_0 = 1$. Furthermore, we also let $f = (f_1, f_2, f_3, f_4)^t$ be the vector field of the system so that we write

$$
\begin{aligned}
\frac{dx_1}{dt} =&\beta_{pv}x_4\,(V_r^*-x_1)-(\gamma_v+\mu_v)(V_r^*-x_1)-\omega x_2-\Lambda := f_1,\\
\frac{dx_2}{dt} =&\beta_{pv}x_4\,(V_r^*-x_1)-(\gamma_v+\mu_v)x_2-\omega x_2 := f_2,\\
\frac{dx_3}{dt} =&-r(P_r^*-x_3)+m(P_r^*-x_3+x_4)(P_r^*-x_3)+\beta_{vp}x_2(P_r^*-x_3) := f_3,\\
\frac{dx_4}{dt} =&rx_4-m(P_r^*-x_3+x_4)x_4+\beta_{vp}x_2(P_r^*-x_3)-(\alpha+\delta)x_4 := f_4.
\end{aligned}
\tag{C.1}
$$

The disease-free equilibrium of (C.1), which corresponds to E_{DFE} is $x^* = (0,0,0,0)^t$. The Jacobian matrix of the right hand of system (C.1) at x^* is

$$
J(x^*) = \begin{pmatrix}
-(\gamma_v+\mu_v) & -\omega & 0 & \dfrac{(\alpha+\delta)(\gamma_v+\mu_v+\omega)}{\beta_{vp}P_r^*}\\
0 & -(\gamma_v+\mu_v+\omega) & 0 & \dfrac{(\alpha+\delta)(\gamma_v+\mu_v+\omega)}{\beta_{vp}P_r^*}\\
0 & \beta_{vp}P_r^* & -r & r\\
0 & \beta_{vp}P_r^* & 0 & -(\alpha+\delta)
\end{pmatrix}.
\tag{C.2}
$$

We see that 0 is a simple eigenvalue of $J(x^*)$, and we go further to find the right eigenvector w, and the left eigenvector, v, which are given by

$$w = \left(\frac{\alpha+\delta}{\beta_{vp}P_r^*}, \frac{\alpha+\delta}{\beta_{vp}P_r^*}, \frac{r+\alpha+\delta}{r}, 1\right)^t,\ \text{and}\ v = (0, \beta_{vp}P_r^*, 0, \gamma_v+\mu_v+\omega)^t,$$

respectively. Algebraic calculations give

$$a = \sum_{k,i,j=1}^{4} v_k w_i w_j \frac{\partial^2 f_k}{\partial x_i \partial x_j}(0,0) = -\frac{2(\gamma_v + \mu_v + \omega)(\alpha + \delta)^2}{m P_r^*},\ b = \sum_{k,i=1}^{4} v_k w_i \frac{\partial^2 f_k}{\partial x_i \partial \phi}(0,0) = \beta_{vp} P_r^* V_r^*.$$

Since $a < 0$ and $b > 0$, the following conclusion holds. When ϕ passes from negative to positive (equivalently $\mathcal{J}_0$ crosses 1), the stability of E_{DFE} changes from stable to unstable and there exists at least one endemic equilibrium which is locally asymptotically stable for $\mathcal{J}_0 > 1$. $\square$